Protection of a non-Fermi liquid by spin-orbit interaction

T. K. T. Nguyen[1] and M. N. Kiselev[2]
[1]*Institute of Physics, Vietnam Academy of Science and Technology, 10 Dao Tan, Hanoi, Vietnam*
[2]*The Abdus Salam International Centre for Theoretical Physics, Strada Costiera 11, I-34151 Trieste, Italy*
(Received 1 April 2015; published 27 July 2015)

We show that a thermoelectric transport through a quantum dot–single-mode quantum point contact nanodevice demonstrating pronounced fingerprints of nonFermi liquid (NFL) behavior in the absence of external magnetic field is protected from magnetic field NFL destruction by strong spin-orbit interaction (SOI). The mechanism of protection is associated with the appearance of additional scattering processes due to lack of spin conservation in the presence of both SOI and small Zeeman field. The interplay between in-plane magnetic field $\vec{B}$ and SOI is controlled by the angle between $\vec{B}$ and $\vec{B}_{\rm SOI}$. We predict strong dependence of the thermoelectric coefficients on the orientation of the magnetic field and discuss a window of parameters for experimental observation of NFL effects.

DOI: 10.1103/PhysRevB.92.045125 PACS number(s): 73.23.Hk, 73.50.Lw, 72.15.Qm, 73.21.La

I. INTRODUCTION

The paradigm of Landau Fermi liquid (FL) [1] is one of the cornerstones of modern condensed matter theory. Based on the concepts of quasiparticles—well-defined excitations whose energy in the long-wave limit is greater than their decay rate—the FL theory successfully explains the behavior of normal and superconducting metals giving universal predictions for thermodynamic and transport properties [2]. The FL phenomenology is justified in many microscopic models describing interacting fermions in and out of equilibrium. However, there are several cases where a violation of the FL picture is observed experimentally (e.g., in strongly correlated electron systems such as heavy fermion compounds [3], unconventional superconductors [2], and quantum transport through nanostructures [4,5]). The pronounced non-Fermi liquid (NFL) behavior of these systems is attributed to a breakdown the quasiparticle concept: The decay rate of low-energy excitations becomes greater than the energy of the excitations itself.

While the fingerprints of NFL physics in thermodynamics of strongly correlated systems and quantum transport had been seen experimentally [3,5], it is also generally accepted that the NFL picture is extremely sensitive to variation of external parameters being unstable against the FL ground state. Thus, the stability of the NFL domain and the possibility to observe strong deviations from the Landau FL paradigm poses major challenges including the development of theoretical models and predictions for the stabilization of NFL states. Important questions are as follows: Is it possible at all to protect unstable NFLs? What are the physical observables which demonstrate the most pronounced manifestation of the NFL physics?

In this paper we present an example based on a window of parameters within which the observation of strong deviation from the FL picture can be protected and extended by effects of strong spin-orbit interaction (SOI). The physical observables we consider in this work are thermoelectric coefficients of a nanodevice (Fig. 1). Our theoretical model justifying NFL behavior is a two-channel Kondo (2CK) model [6–8]. While the scattering of single orbital channel electrons on a resonance quantum impurity itself leads to strong modification of the thermoelectric transport properties within the Landau FL paradigm through strong renormalization of the FL energy scale [9–11], the detour from the FL picture is predicted to change completely both electric [12–15] and thermoelectric transports [16,17]. For example, one of the manifestations of the NFL behavior in quantum transport is associated with the logarithmic enhancement of the thermoelectric power [16] in the situation when the 2CK model originates from the charge Kondo effect in a single mode quantum point contact (QPC)–quantum dot (QD) setup tuned by gate voltages to the Coulomb blockade (CB) peak regime [12–16]. In that case two channels are the electron spin degrees of freedom while the almost transparent QPC (weak back-scatterer) works as a quantum impurity. The 2CK physics is known to be unstable with respect to any effects which can potentially break (statically or dynamically) the symmetry between the channels [5,17]. In particular, it has been shown that the effects associated with time-reversal symmetry breaking (TRS) due to an external magnetic field restore the FL properties at temperatures below $T_{\rm eff}$ tunable by the field [17]. The universality class of the unstable 2CK model than changes to a single channel Kondo problem (1CK). *Fully screened* 1CK is characterized by stable *local* FL properties. Therefore, while being very attractive from the theoretical point of view, the 2CK physics suffers from serious experimental obstacles [4,5,18] impeding a direct observation of NFL behavior.

The paper is organized as follows: We describe possible experimental setup for observing the NFL transport in Sec. II. A theoretical model accounting for the interplay between SOI, external magnetic field, and effects of Coulomb blockade in quantum dot is presented in Sec. III. We discuss the solution of the one-dimensional (1D) quantum-mechanical scattering problem in the presence of strong SOI in Sec. IV. An effective model describing a low-energy physics of the problem and its exact solution is presented in Sec. V. The transport coefficients computed with the help of the exact solutions are discussed in Sec. VI. Section VII is devoted to discussion of the key results of the paper including estimation for the parameters and definition of the conditions necessary for experimental observations of the NFL physics. Summary and Conclusions are given in Sec. VIII. Details of derivation of the effective model are presented in Appendix.

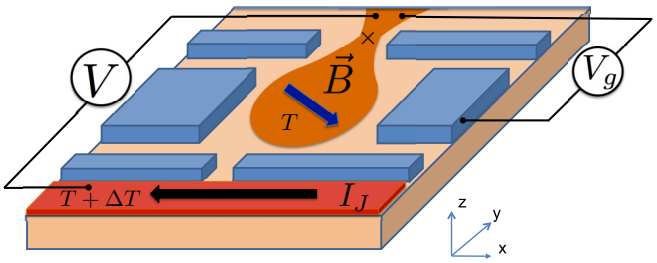

FIG. 1. (Color online) Typical setup for thermoelectric measurements: "cold" contact (light orange area) at reference temperature T, quantum dot–quantum point contact electrostatically defined by gates (blue boxes), separated by a tunnel barrier from a "hot" (deep orange) contact at temperature $T+\Delta T$. The voltage V is applied across the device for zero current measurements (see text for the details).

II. PROPOSED EXPERIMENTAL SETUP

We consider a two-terminal nanodevice (see Fig. 1) designed to be used for thermoelectric measurements [19,20]. The QD–QPC contains 2-d electron gas (2DEG) confined in the z direction (light orange area on the Fig. 1). The open QPC connects it to the drain at the reference temperature T. We assume that the Rashba SOI [21,22] (caused by the gradient of the confining potential in the z direction) leads to appreciable effects which we will discuss in this paper. The source is separated from the QD by a tunnel barrier with low transparency $|t| \ll 1$. The temperature of the source (deep orange) is adjusted by the Joule heat controlled by the current I_J flowing along the lead (black arrow). The temperature difference ΔT across the tunnel barrier is assumed to be small compared to the reference temperature T to guarantee the linear response operation regime for the device. The QD is electrostatically controlled by two plunger gates (blue rectangles) to adjust the size of the electron island. The device is operated in the steady state of zero source-drain current $I_{\rm sd} = 0 = G\Delta V_{\rm th} + G_T\Delta T$, controlled by applying a thermo-voltage $\Delta V_{\rm th}$ between the source and the drain. The QPC (denoted by the cross in the light orange area) is tuned to the single mode regime characterized by a controllable small reflectivity $|r| \ll 1$. Under this assumption and neglecting the resistance of the "metallic" QD we assume that the voltage difference $\Delta V_{\rm th}$ arises across the tunnel barrier between the source and QD. The transport coefficients, electric conductance G and thermoelectric coefficient G_T (measured independently), define the thermoelectric power (TP) S:

$$G_T = \frac{\partial I_{\rm sd}}{\partial \Delta T}, \quad G = \frac{\partial I_{\rm sd}}{\partial V}, \quad S = -\frac{\Delta V_{\rm th}}{\Delta T}\bigg|_{I_{sd}=0} = \frac{G_T}{G}.$$

We assume that the magnetic field (blue arrow) is applied parallel to the plane of 2DEG to avoid orbital effects.

III. THEORETICAL MODEL

The theoretical description of setup (see Fig. 1) is formulated in terms of the Hamiltonian:

$$H = H_s + H_d + H_{\rm tun} + H_z. \tag{1}$$

Here H_s and H_d are the Hamiltonians of the source ("hot" contact) and the drain ("cold" contact), respectively. $H_{\rm tun}$ describes tunneling between the source and the drain and H_z accounts for the Zeeman effect in both contacts. We assume that the source can be described by a standard FL approach,

$$H_s = \sum_{k,\sigma} \epsilon_{k\sigma} c^\dagger_{k\sigma} c_{k\sigma}, \tag{2}$$

where $c^\dagger$ and c are creation/annihilation operators of quasiparticles (we adopt a system of units $\hbar = k_B = 1$). The drain $H_d = H_c + H_{\rm QPC}$ includes the Coulomb blockaded QD described by charging Hamiltonian H_c and QPC represented by

$$H_{\rm QPC} = H_0 + H_{\rm SOI} + H_{\rm BS}. \tag{3}$$

We assume that the charge $\hat{Q} = e(\hat{n}_s + \hat{n}_d)$ in the QD is weakly quantized (mesoscopic CB regime [27]) and controlled by the gate voltage V_g:

$$H_c = E_c[\hat{n}_s + \hat{n}_d - N(V_g)]^2, \tag{4}$$

where $\hat{n}_s$ and $\hat{n}_d$ are the operators of the number of electrons that entered the dot through the source and the drain, respectively, and $E_c \sim e^2/L_{\rm QD}$ is the charging energy of QD with geometric size $L_{\rm QD}$. Below we ignore effects associated with finite mean-level spacing in the dot. While charge is only weakly quantized in the mesoscopic CB regime, the spin remains a good quantum number in the absence of SOI. However, when the SOI is present, two spin sub-bands are split *horizontally in k space* and while spin is no more conserved, the sub-band index characterizes quantized states instead. The single mode QPC being a short quantum wire can be viewed as a 1D electron system in the presence of Rashba SOI [23–26] $H_{\rm SOI} = \alpha_R[\vec{k} \times \vec{n}_z] \cdot \vec{\sigma}$:

$$H_0 = -iv_F \sum_{\lambda\sigma} \lambda \int_{-\infty}^{\infty} dy \Psi^\dagger_{\lambda,\sigma}(y)\partial_y \Psi_{\lambda,\sigma}(y), \tag{5}$$

$$H_{\rm SOI} = \alpha_R k_F \sum_{\lambda\sigma} \lambda \int_{-\infty}^{\infty} dy [\Psi^\dagger_{\lambda,\uparrow}\Psi_{\lambda,\downarrow} + \Psi^\dagger_{\lambda,\downarrow}\Psi_{\lambda,\uparrow}]. \tag{6}$$

We denote here by $\Psi_{\lambda,\sigma}$ the left ($\lambda = -$) and right ($\lambda = +$) movers with spin $\sigma = \uparrow,\downarrow$. The constant α_R characterizes Rashba SOI strength. The k_F and $v_F = k_F/m^*$ correspond to the Fermi momentum and Fermi velocity (here m^* is a fermion's mass). The 1D electron transport through the QPC is along the y axis (see Fig. 1). The Rashba SOI $H_{\rm SOI} = \alpha_R k_y \sigma_x$ is associated with the electric field gradient along the z axis and can be characterized by the effective SOI field $g\mu_B \vec{B}_{\rm SOI}/2 = \alpha_R k_F \vec{e}_x$ perpendicular to the direction of electron transport (g is the Lande factor; μ_B is the Bohr magneton). Notice that the SOI field alone does not lead to the TRS breaking.

The backscattering (BS) Hamiltonian describes a scattering of electrons with momentum transfer $2k_F$ on a nonmagnetic quantum impurity located at the origin and characterized by a short-range potential $V(y)$:

$$H_{\rm BS} = \sum_{\lambda,\sigma} \int dy \Psi^\dagger_{\lambda,\sigma}(y) V(y) \Psi_{\bar{\lambda},\sigma}(y) e^{-2i\lambda k_F y}. \tag{7}$$

The Hamiltonian $H_{\rm tun}$ represents the weak tunneling $|t_k| = |t| \ll 1$ of the electrons from the left contact to QD:

$$H_{\rm tun} = \sum_{k\lambda\sigma} [t_k c^\dagger_{k\sigma} \Psi_{\lambda\sigma}(-\infty) + \text{H.c.}]. \quad (8)$$

The Zeeman Hamiltonian H_z describes the effects of the external magnetic field $H_z = -g\mu_B \vec{B}(\vec{s}_s + \vec{s}_d)$, where $\vec{s}_s$ and $\vec{s}_d$ are the spin densities of electrons in the source and drain, respectively. We consider a situation when both sizes of the QD ($L_{\rm QD}$) and QPC ($L_{\rm QPC}$) are small compared to the SOI length scale $L_{\rm QD} \sim L_{\rm QPC} \ll l_{\rm SOI} = 1/(m^*\alpha_R)$. Since the effective energy scale determining the behavior of the transport coefficients of the model (2)–(8) which will be referred to below as the Kondo temperature T_K is [14] $\sim E_c$ (see Appendix), the condition $l_{\rm SOI} \gg L_{\rm QD}$ is equivalent to $g\mu_B B_{\rm SOI} \ll T_K$ (see a discussion about interplay between the Kondo effect and SOI in Ref. [28]). We also assume that the SOI effects in the QD are already taken into account by using the approach developed in Ref. [29].

IV. SCATTERING IN THE PRESENCE OF SOI AND MAGNETIC FIELD

We consider the 1D scattering problem in the presence of SOI [21] and Zeeman field applied parallel to the plane of 2DEG. The Hamiltonian is given by

$$\mathcal{H} = \mathcal{H}_0 + V(y) = \frac{k^2}{2m^*} + \alpha_R \sigma_x k - \gamma \vec{\sigma}\cdot\vec{B} + V(y). \quad (9)$$

The short-range potential $V(y)$ describes a nonmagnetic impurity located at the origin [24,25]. The electron's transport is along the y direction, $k = k_y$. Angle φ characterizes the orientation of magnetic field $\vec{B}$ with respect to the y axis (see Fig. 2, left bottom panel insert).

The kinetic energy term of (9) is given by

$$\mathcal{H}_0 = \begin{pmatrix} \frac{k^2}{2m^*} & \alpha_R k + i\gamma B e^{i\varphi} \\ \alpha_R k - i\gamma B e^{-i\varphi} & \frac{k^2}{2m^*} \end{pmatrix}. \quad (10)$$

The Hamiltonian $\mathcal{H}_0$ is promptly diagonalized in k space. The eigenvalues (spectra) describe two sub-bands ($\nu = +$ and $\nu = -$) split both horizontally due to the SOI and vertically due to the Zeeman effect (Fig. 2):

$$E_\pm(k) = \frac{k^2}{2m^*} \pm \sqrt{(\alpha_R k)^2 + (\gamma B)^2 - 2\alpha_R \gamma k B \sin\varphi}. \quad (11)$$

(We use the short-hand notation $\gamma = g\mu_B/2$.) In the presence of both fields there are two sub-bands while the spin polarization changes continuously as one moves from one Fermi point to the other along each sub-band. We assume that magnetic field is applied parallel to the plane of the 2DEG to decouple it from the orbital degrees of freedom and concentrate on the Zeeman effect only. The angle φ characterizes the orientation of $\vec{B}$ with respect to the axis of 1D transport (y). The spectra for $\varphi = 0$, perpendicular orientation of $\vec{B}$ and $\vec{B}_{\rm SOI}$, describe the situation when magnetic field $\vec{B}$ is oriented *along* the direction of the transport. If B is larger than $B_{\rm SOI}$, the most important effects on thermoelectric transport are due to the Zeeman splitting of two sub-bands (Fig. 2, upper left panel) [17]. In that limit the effects of B are associated with breaking of the

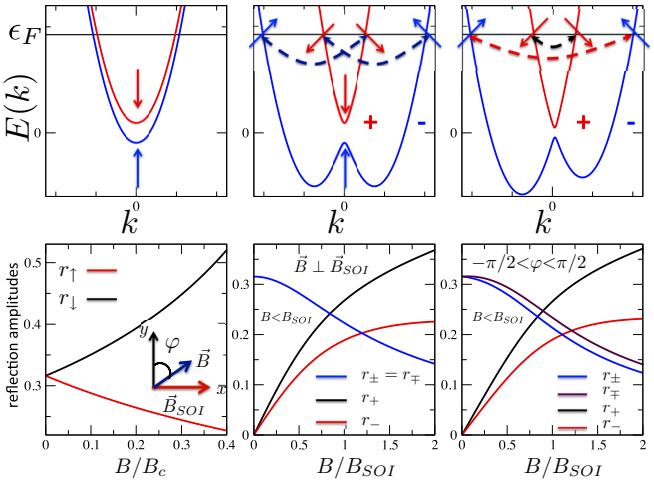

FIG. 2. (Color online) (Top panels) Two sub-band spectra: (left) Zeeman splitting in the absence of SOI; (center) $\vec{B} \perp \vec{B}_{\rm SOI}$, angle between magnetic field and y direction $\varphi = 0$; (right) arbitrary angle $-\pi/2 < \varphi < \pi/2$. (Bottom panels) Magnetic field dependence of reflection amplitudes $|r_{\mu\nu}|$ for the spectra shown in top panels. For illustration we performed all calculations with model barrier $V(y) = V_0 \exp(-|y|/L_{\rm QPC})$, $k_{0F} L_{\rm QPC} = 3.6$, and height of the barrier V_0 is tuned to get $r^2_{0\to} = 0.1$ (see details in the text). Insert shows relative orientation of $\vec{B}$ and $\vec{B}_{\rm SOI}$.

channel symmetry, $|r_\uparrow| \neq |r_\downarrow|$ (Fig. 2, lower left panel) which is crucial for the fate of NFL [17]. For the case $B < B_{\rm SOI}$ we distinguish two cases: (i) $\varphi = 0$ (Fig. 2, central panel) and (ii) $-\pi/2 < \varphi < \pi/2, \varphi \neq 0$ (Fig. 2, right panel). Since the orbital effects are negligible for small magnetic fields if $B < B_{\rm SOI}$, the case (i) $\varphi = 0$ (Fig. 2, central panel) can also be realized when magnetic field is perpendicular to the plane of 2DEG. Besides, the theory discussed in the paper is also applicable when both Rashba and Dresselhaus SOI [21,22] are present. The transport coefficients for the generic situation of the in-plane B field are fully determined by the angle $\Phi = \varphi_0 - \varphi$ between $\vec{B}$ and $\vec{B}_{\rm SOI}$, where φ_0 (φ) are the angles between $\vec{B}_{\rm SOI}$ ($\vec{B}$) and axis of 1D motion, respectively.

The eigenfunctions of H_{1d} are momentum-dependent spinors $\Psi_\nu(y) = e^{ik\cdot y}\chi_\nu(k)$,

$$\chi_\pm(k) = \frac{1}{\sqrt{2}} \begin{pmatrix} \pm i e^{-i\vartheta(k)} \\ 1 \end{pmatrix}, \quad (12)$$

where

$$\vartheta(k) = \arctan\left(\frac{\alpha_R k - \gamma B \sin\varphi}{\gamma B \cos\varphi}\right). \quad (13)$$

The four reflection amplitudes in the first order of the backscattering potential are determined by $2k_F$ momentum transfer and given by the matrix elements of $V(y)$ in spinor basis Ψ_ν. The diagonal matrix elements,

$$|r_{\mu\mu}| = \left| \frac{V\left(k^\mu_{F+} - k^\mu_{F-}\right)}{v_{0F}} \cos\left(\frac{\vartheta\left(k^\mu_{F+}\right) - \vartheta\left(k^\mu_{F-}\right)}{2}\right)\right| \quad (14)$$

characterize the intraband scattering (we shall use the short-hand notations $|r_{\mu\mu}| \equiv |r_\mu|$ below). Here $k^\mu_{F+} > 0$ and $k^\mu_{F-} < 0$ stand for the right and left Fermi points of a sub-band μ, respectively, $v_{0F} \sim (m^* a)^{-1}$ originates from the high energy

cutoff, and a is a lattice constant. The off-diagonal matrix elements ($|r_{+-}| \equiv |r_{\pm}|$ and $|r_{-+}| \equiv |r_{\mp}|$):

$$|r_{\mu\nu}| = \left| \frac{V\left(k^{\mu}_{F+} - k^{\nu}_{F-}\right)}{v_{0F}} \sin\left(\frac{\vartheta\left(k^{\mu}_{F+}\right) - \vartheta\left(k^{\nu}_{F-}\right)}{2} \right) \right| \quad (15)$$

describe the interband scattering.

The backscattering Hamiltonian (7) in the basis of eigenfunctions (12) casts the following form:

$$H_{\rm BS} = v_F \sum_{\lambda\mu\nu} |r_{\mu\nu}| [\Psi^{\dagger}_{\lambda,\mu}(0)\Psi_{\bar{\lambda},\nu}(0) + \text{H.c.}]. \quad (16)$$

Let us analyze various limits of the backscattering corresponding to different orientation of the in-plane magnetic field $\vec{B}$ in the regime of strong interplay with the effects of SOI.

For the most generic case of interplay between SOI and Zeeman magnetic field there exist four independent scattering processes resulting in four different reflection amplitudes (Fig. 2, right lower panel). The reflection amplitudes for the intraband scattering $|r_+|$ and $|r_-|$ (black and red dashed arrow on Fig. 2, right upper panel) in the first order of the backscattering potential are proportional to the amplitude of B [25],

$$|r_{+/-}| = r_0 \left[\frac{k_{0F}}{k_{0F} \mp \delta} \right] \left(\frac{B}{B_{\rm SOI}} \right) \cos\varphi, \quad (17)$$

where k_{0F} is the Fermi momentum at zero splitting ($\delta = 0$), $\delta = m^*\alpha_R$, $r_0 \propto |V(2k_{0F})m^*a| \ll 1$ is a coefficient characterizing the transparency of the barrier. The intraband scattering completely suppresses for $\varphi = \pi/2$ since the angle $\vartheta(k_{F\pm}) = \pm\pi/2$ and the eigenfunctions do not depend on B. The intraband reflection amplitudes $|r_+| = |r_-| = 0$ while interband ($|r_{\pm}|, |r_{\mp}|$) $\neq 0$. Thus, for $\varphi = \pi/2$ we have only two nonzero reflection amplitudes $|r_{\pm}|$ and $|r_{\mp}|$ and therefore the thermoelectric transport can be described by equations of Ref. [17] if replacing $|r_{\uparrow}| \to |r_{\pm}|$ and $|r_{\downarrow}| \to |r_{\mp}|$.

The interband scattering amplitudes (blue dashed arrows on central upper panel of Fig. 2) for the case $-\pi/2 < \varphi < \pi/2$ are given by

$$|r_{\pm/\mp}| = r_0 \left[1 \mp b \left(\frac{B \sin\varphi}{B_{\rm SOI}} \right) - c(\varphi) \left(\frac{B}{B_{\rm SOI}} \right)^2 \right]. \quad (18)$$

Here coefficients $(b, c(\varphi)) \sim 1$ depend on the geometry of the QPC. One can see that for $\varphi = 0$, the scattering term linear in B (linear Zeeman effect) disappears and additional symmetry $|r_{\pm}| = |r_{\mp}|$ emerges (Fig. 2, central panel). The reflection amplitudes depend on magnetic field quadratically (quadratic Zeeman effect). Thus, the scattering Hamiltonian in that case contains three independent scattering parameters.

V. EFFECTIVE MODEL

We recapitulate briefly the main steps of the derivation of transport coefficients (for details see Appendix): (i) we bosonize the 1D Hamiltonian (5)–(7) using a standard approach [31,32]. The effective bosonic Hamiltonian gives us a boundary sine-Gordon (BSG) model [32] with four different backscattering amplitudes. The high-T results are obtained by perturbative expansion (in reflection amplitudes) around the strong-coupling fixed point of the model. (ii) The nonperturbative results in the low-T regime are obtained by the re-fermionization procedure through mapping the BSG model onto the effective Anderson model [12,15–17]. (iii) The effects of the Zeeman field at the QPC resulting in TRS breaking caused by the asymmetry of reflection amplitudes [17] are accounted by a magnetic-field-dependent resonance width Γ at the CB peaks [17]. The resonance width Γ in the presence of the Zeeman field remains finite for a whole range of the gate voltages, cuts the temperature-dependent logarithm, and therefore restores FL properties. The width Γ (Refs. [12,14,32]) is attributed to a *single local Majorana mode* interacting with a *single* mode of chiral fermions [12,16] in the theory containing only two (intraband) scattering processes. The scattering on quantum impurity in the presence of SOI and Zeeman fields involves four "$2k_F$" processes which can be accounted for by *two local Majorana modes* interacting with *four* modes of *two* species of the chiral fermions. As a result, two different resonance widths enter the transport coefficients. The interplay between two widths associated with inter- and intraband processes leads to remarkable effects in thermoelectric transport.

The effective Anderson model which describes a hybridization of two local Majorana fermions η_1 and η_2 with two species of *chiral* fermions (see Appendix) is a direct generalization of [12,14,16,17] for a case of interplay between Zeeman and SOI fields:

$$\begin{aligned} H_{\tau}(t) = \int_{-\infty}^{\infty} dk \Big[& \sum_{\alpha=1,2} (k \cdot v_F) c^{\dagger}_{\alpha,k} c_{\alpha,k} \\ & - \sqrt{2}(\omega_{s\tau}(t)\eta_1(c_{1,k} - c^{\dagger}_{1,k}) - i\omega_{a\tau}(t)\eta_1(c_{1,k} + c^{\dagger}_{1,k}) \\ & + \omega_{ms\tau}(t)\eta_2(c_{2,k} - c^{\dagger}_{2,k}) - i\omega_{ma\tau}(t)\eta_2(c_{2,k} + c^{\dagger}_{2,k})) \Big], \end{aligned} \quad (19)$$

where following Ref. [16] we define

$$\begin{aligned} \omega_{s/a\,\tau}(t) &= \Omega_{s/a} f_{s/a\,\tau}(t), \\ \omega_{ms/ma\,\tau}(t) &= \Omega_{ms/ma} f_{s/a,\,\tau}(t), \end{aligned} \quad (20)$$

with

$$\begin{aligned} \Omega_{s/a} &= \sqrt{\frac{v_F E_c e^C}{2\pi^3}} \big| |r_+| \pm |r_-| \big|, \\ \Omega_{ms/ma} &= \sqrt{\frac{v_F E_c e^C}{2\pi^3}} \big| |r_{\pm}| \pm |r_{\mp}| \big|, \end{aligned} \quad (21)$$

and the time-dependent functions,

$$f_{s/a\,\tau} = (-1)^{n_{\tau}(t)} \text{Re/Im}[\exp\{i(\delta\chi_{\tau}(t) - \pi N)\}]. \quad (22)$$

Function $\delta\chi_{\tau}(t)$ describes the deviation of the phase of the charge mode mean value from $\pi n_{\tau}(t)$ (Ref. [16]):

$$\delta\chi_{\tau}(t) \approx \frac{\pi^2 T}{2E_c} (\cot[\pi T(t-\tau)] - \cot[\pi T t]), \quad (23)$$

where N is a function of a gate voltage V_g: N is integer in the Coulomb blockade valleys and half-integer in the Coulomb blockade peaks, $n_{\tau}(t) = \theta(t)\theta(\tau - t)$ ($\theta(t)$ is a step function), and $C \approx 0.577$ is the Euler's constant.

The original Matveev model [12] corresponds to the case $\Omega_a = \Omega_{ma} = \Omega_{ms} = 0$ and describes a *single Majorana fermion* η_1 coupled to the *odd* combination of creation/annihilation operators of *chiral* fermions. In contrast to the conventional Anderson model which preserves $U(1)$ symmetry, the model [12,14] is characterized by Z_2 symmetry instead. As a result, the NFL properties associated with the two-channel Kondo physics emerge. The NFL behavior of the two-channel Kondo model are attributed to the *overscreened* regime realized when the number of orbital channels $\mathcal{N}$ exceeds twice the spin of a quantum impurity. As it was shown in Ref. [17], the Zeeman in-plane magnetic field restores the $U(1)$ symmetry through appearance of nonzero Ω_a and therefore leads to the restoration of the FL behavior characteristic for the single-channel fully screened Kondo model in both thermodynamic [15] and transport [17] coefficients. The Kondo temperature T_K is of the order of the charging energy E_c (see Appendix). The effective Hamiltonian (19) describing scattering in the presence of both Zeeman and SOI fields has a structure of two copies of the two-channel Kondo model where coupling constants $\omega_{i\tau}$ depend on the magnetic field. Thus, when all reflection amplitudes are different, the model (19) is characterized by generic FL properties. However, if *accidental* degeneracy fine-tuned by the orientation of the in-plane magnetic field appears, one of the nonidentical copies of the two-channel Kondo model preserves the NFL properties.

The effects of interplay between the backscattering at the QPC and Coulomb interaction in the QD can be accounted by the correlator $K(\tau) = \langle T_\tau F(\tau) F^\dagger(0)\rangle$ (see details in Refs. [16,17]). The operator $F(\tau)$ accounts for the *weak charge quantization* in the *mesoscopically Coulomb blockaded* QD. Following Ref. [16] we define the charge of QD $\hat{Q} = e(\hat{n}_\tau + \hat{n}_d)$, where $\hat{n}_\tau$ is an integer valued operator which commutes with the annihilation operator of the electron in the dot at the position of the source Ref. [14]. Since by definition $[F(\tau),\hat{n}_\tau] = F(\tau)$, the role of operator $F(\tau)$ is to account for the effects of interaction in QD: $\Psi_\lambda(\tau) = F(\tau)\Psi_{0\lambda}(\tau)$ where Ψ_λ and $\Psi_{0\lambda}$ correspond to interacting and noninteracting left/right fermions, respectively. Thus, the dressed Green's function (GF) $\mathcal{G}(\tau) = -\langle T_\tau \Psi_\lambda(\tau)\Psi^\dagger_\lambda(0)\rangle$ and free fermionic Green's function $G_0(\tau) = -\langle T_\tau \Psi_{0\lambda}(\tau)\Psi^\dagger_{0\lambda}(0)\rangle = -\pi\nu_0 T/\sin(\pi T\tau)$ are connected [16] by the simple relation $\mathcal{G}(\tau) = K(\tau)G_0(\tau)$ (here ν_0 is a density of states in QD). The transport coefficients of the model are determined by the Green's function $\mathcal{G}$ (see next section).

In order to compute the Green's function $\mathcal{G}$ (or, equivalently, compute the correlator K) we define the operator $U_\tau = (-1)^{d^\dagger d}$ where $d = (\eta_1 + i\eta_2)/\sqrt{2}$ and $d^\dagger = (\eta_1 - i\eta_2)/\sqrt{2}$. We keep notations of the Matveev and Andreev work Ref. [16] for $U_\tau = 2i\eta_2\eta_1$. Notice that the "spin" and charge are completely disentangled in the correlator $K(\tau) = K_c(\tau)K_s(\tau)$.

While $K_c(\tau) = \pi^2 T e^{-C}/(2E_c|\sin(\pi T\tau)|)$ (see Refs. [14,16] for details of calculations), the $K_s(\tau)$ in zeroth order in $H_\tau(t) - H_{\tau=0}(t)$ is defined by the correlator,

$$K_s^{(0)}(\tau) = \langle T_t U(\tau)U(0)\rangle_0. \tag{24}$$

Here $\langle ...\rangle_0$ denotes an averaging with (19) taken at $\tau = 0$. (Notice obvious correspondence $\eta_1 \to \sigma_x/\sqrt{2}$, $\eta_2 \to \sigma_y/\sqrt{2}$, and $2i\eta_2\eta_1 \to \sigma_z$, where σ_i are spin $s = 1/2$ operators ($i = x,y,z$). Therefore, $K_s^0(\tau) = \langle T_t \sigma_z(\tau)\sigma_z(0)\rangle$.)

The first nonvanishing order in $H_\tau(t) - H_{\tau=0}(t)$ correction to the correlator $K_s(\tau)$ is given by

$$K_s^{(1)}(\tau) = -\int_0^{1/T} dt\,\langle T_t H'_\tau(t)U(\tau)U(0)\rangle_0, \tag{25}$$

where the Hamiltonian $H'_\tau(t)$ has the form,

$$\begin{aligned} H'_\tau(t) = -2i\delta\chi_\tau(t)(&\Omega_s \sin(\pi N)\eta_1\varsigma_1 - \Omega_a\cos(\pi N)\eta_1\zeta_1 \\ &+ \Omega_{ms}\sin(\pi N)\eta_2\varsigma_2 - \Omega_{ma}\cos(\pi N)\eta_2\zeta_2). \end{aligned} \tag{26}$$

Here we define four additional Majorana fermions ($\alpha = 1,2$) through a k-Fourier transform of the even/odd combinations of creation/annihilation operators of two species of *chiral* fermions $c_{\alpha,k}$ taken at the position of the quantum impurity $y = 0$:

$$\begin{aligned} \zeta_\alpha &= \int_{-\infty}^{\infty} dk\,\zeta_{\alpha k} = \frac{1}{\sqrt{2}}\int_{-\infty}^{\infty} dk(c_{\alpha,k} + c^\dagger_{\alpha,k}), \\ \varsigma_\alpha &= \int_{-\infty}^{\infty} dk\,\varsigma_{\alpha k} = \frac{1}{i\sqrt{2}}\int_{-\infty}^{\infty} dk(c_{\alpha,k} - c^\dagger_{\alpha,k}). \end{aligned} \tag{27}$$

In order to compute the correlators (24) and (25) we apply the Wick's theorem to the product of an even number of fermions and express the result in terms of the products of the single-particle GFs. The imaginary time (Matsubara) GFs form a 6×6 matrix with 21 independent components (six diagonal and 15 off-diagonal):

$$\begin{aligned} &G^{\eta\eta}_{\mu\nu}(\tau) = -\langle T_\tau \eta_\mu(\tau)\eta_\nu(0)\rangle, \quad G^{\zeta\zeta}_{\mu\nu}(\tau) = -\langle T_\tau \zeta_\mu(\tau)\zeta_\nu(0)\rangle, \\ &G^{\varsigma\varsigma}_{\mu\nu}(\tau) = -\langle T_\tau \varsigma_\mu(\tau)\varsigma_\nu(0)\rangle, \quad G^{\zeta\varsigma}_{\mu\nu}(\tau) = -\langle T_\tau \zeta_\mu(\tau)\varsigma_\nu(0)\rangle, \\ &G^{\zeta\eta}_{\mu\nu}(\tau) = -\langle T_\tau \zeta_\mu(\tau)\eta_\nu(0)\rangle, \quad G^{\varsigma\eta}_{\mu\nu}(\tau) = -\langle T_\tau \varsigma_\mu(\tau)\eta_\nu(0)\rangle. \end{aligned}$$

The GF s of the quadratic Anderson-type Hamiltonian (19) can be found exactly (e.g., by solving equations of motion for the Majorana fermions). For computing the correlators (24) and (25) we need only six GFs, namely, two diagonal local Majorana's GF (here R denotes the retarded GFs):

$$G^{\eta\eta}_{11,R}(\epsilon) = \frac{1}{\epsilon + i\Gamma_B}, \quad G^{\eta\eta}_{22,R}(\epsilon) = \frac{1}{\epsilon + i\Gamma_A}, \tag{28}$$

and four off-diagonal hybridized GFs:

$$\begin{aligned} G^{\zeta\eta}_{11,R}(\epsilon) &= \frac{\Omega_a \sin(\pi N)2\pi/v_F}{\epsilon + i\Gamma_B}, \\ G^{\varsigma\eta}_{11,R}(\epsilon) &= \frac{\Omega_s \cos(\pi N)2\pi/v_F}{\epsilon + i\Gamma_B}, \\ G^{\zeta\eta}_{22,R}(\epsilon) &= \frac{\Omega_{ma} \sin(\pi N)2\pi/v_F}{\epsilon + i\Gamma_A}, \\ G^{\varsigma\eta}_{22,R}(\epsilon) &= \frac{\Omega_{ms} \cos(\pi N)2\pi/v_F}{\epsilon + i\Gamma_A}. \end{aligned} \tag{29}$$

Here we denote the resonance widths associated with the symmetric and antisymmetric combinations of reflection amplitudes as

$$\begin{aligned} \Gamma_{s/ms} &= \Omega^2_{s/ms}\cos^2(\pi N)4\pi/v_F, \\ \Gamma_{a/ma} &= \Omega^2_{a/ma}\sin^2(\pi N)4\pi/v_F. \end{aligned} \tag{30}$$

Two resonance Kondo widths entering the transport coefficients are given by

$$\Gamma_A = \Gamma_{ms} + \Gamma_{ma}, \quad \Gamma_B = \Gamma_s + \Gamma_a. \tag{31}$$

Notice that 10 GFs, namely $G^{\zeta\zeta}_{\mu\nu}$, $G^{\varsigma\varsigma}_{\mu\nu}$, and $G^{\zeta\varsigma}_{\mu\nu}$ do not depend on the local Majorana fermions describing the quantum impurity. These GF renormalize the correlations between the conduction electrons, but do not enter Eqs. (24) and (25). Another five GFs allowed by the symmetry of the Hamiltonian (19) do not appear in Eqs. (24) and (25) due to specific form of fermionic correlations in the Hamiltonian $H'_\tau(t)$.

VI. TRANSPORT COEFFICIENTS

The thermoelectric coefficient G_T and electric conductance G,

$$G_T = -\frac{i\pi^2 G_L T}{2e}\int_{-\infty}^{\infty}\frac{\sinh(\pi T t)}{\cosh^3(\pi T t)}K\left(\frac{1}{2T}+it\right)dt, \tag{32}$$

$$G = \frac{\pi G_L T}{2}\int_{-\infty}^{\infty}\frac{1}{\cosh^2(\pi T t)}K\left(\frac{1}{2T}+it\right)dt, \tag{33}$$

are here calculated by accounting for interaction effects in the QD through the correlator $K(\tau)$ defined in the previous section. The conductance of the barrier between the source and QD $G_L = 2\pi e^2 \nu_0 \nu_L |t|^2$ is expressed through Fermi's golden rule as a function of the density of states (DoS) of the source ν_L, the DoS of the QD ν_0, and the weak tunneling amplitude $|t|$ (Ref. [30]).

The correlator $K_s^{(0)}(1/(2T)+it)$ defined by (24) is an even function of time. This correlator determines the behavior of the electric conductance G, but does not contribute to G_T:

$$G^{(0)} = \frac{G_L \Gamma_A \Gamma_B e^{-C}}{32\pi T E_c} F_G\left(\frac{\Gamma_A}{T},\frac{\Gamma_B}{T}\right). \tag{34}$$

The equation for the thermoelectric coefficient G_T is given by an odd function $K_s^{(1)}(1/(2T)+it)$ defined by (25):

$$G_T^{(1)} = -\frac{G_L\Gamma_A\Gamma_B \sin(2\pi N)}{6e\pi^2 E_c}\left[\frac{|r_+ r_-|}{\Gamma_B}\ln\left(\frac{E_c}{T+\Gamma_B}\right)F\left(\frac{\Gamma_B}{T},\frac{\Gamma_A}{T}\right)+\frac{|r_\pm r_\mp|}{\Gamma_A}\ln\left(\frac{E_c}{T+\Gamma_A}\right)F\left(\frac{\Gamma_A}{T},\frac{\Gamma_B}{T}\right)\right]. \tag{35}$$

The ratio of G_T and G defines the thermoelectric power:

$$S = -\frac{16e^C \sin(2\pi N)T}{3e\pi}\left[\frac{|r_+ r_-|}{\Gamma_B}\ln\left(\frac{E_c}{T+\Gamma_B}\right)\frac{F\left(\frac{\Gamma_B}{T},\frac{\Gamma_A}{T}\right)}{F_G\left(\frac{\Gamma_A}{T},\frac{\Gamma_B}{T}\right)}+\frac{|r_\pm r_\mp|}{\Gamma_A}\ln\left(\frac{E_c}{T+\Gamma_A}\right)\frac{F\left(\frac{\Gamma_A}{T},\frac{\Gamma_B}{T}\right)}{F_G\left(\frac{\Gamma_A}{T},\frac{\Gamma_B}{T}\right)}\right]. \tag{36}$$

The functions F_G and F universally depend on the ratio of the resonance Kondo widths Γ_A, Γ_B and the temperature:

$$F_G(x,y) = \int_{-\infty}^{\infty}\int_{-\infty}^{\infty} dz dz' \frac{[(z+z')^2+\pi^2]}{[(z')^2+x^2][z^2+y^2]}\frac{1}{\cosh\left(\frac{z}{2}\right)\cosh\left(\frac{z'}{2}\right)\cosh\left(\frac{z+z'}{2}\right)}, \tag{37}$$

$$F(x,y) = \int_{-\infty}^{\infty}\int_{-\infty}^{\infty} dz dz' \frac{z(z+z')[(z+z')^2+\pi^2]}{[z^2+x^2][(z')^2+y^2]}\frac{1}{\cosh\left(\frac{z}{2}\right)\cosh\left(\frac{z'}{2}\right)\cosh\left(\frac{z+z'}{2}\right)}. \tag{38}$$

VII. RESULTS AND DISCUSSION

A. Four main regimes of thermoelectric transport

The nonperturbative equation for the resonance width Γ related to the interband scattering (30) and (31) demonstrates a weak dependence of Γ on the magnetic field away from the CB peaks (see Fig. 3, left panel):

$$\Gamma_A \propto \Gamma_0\left[\left(1-\Lambda_A^2\right)\cos^2(\pi N)+\Delta_A^2\right], \tag{39}$$

where $\Gamma_0 = r_0^2 E_c$, $\Delta_A(B,\varphi) = b(B/B_{\rm SOI})\sin\varphi$, and $\Lambda_A^2 = \Delta_A^2 + 2c(\varphi)(B/B_{\rm SOI})^2$.

In contrast, the resonance width Γ associated with the intraband scattering (30) and (31) strongly depends on B at all gate voltages:

$$\Gamma_B \propto \Gamma_0\left[\left(1-\Delta_B^2\right)\cos^2(\pi N)+\Delta_B^2\right]\left(\frac{B\cos\varphi}{B_{\rm SOI}}\right)^2. \tag{40}$$

The $\Gamma_B^{\min} \equiv \Gamma_B(N=\frac{1}{2}) \propto \Gamma_0(B\cos\varphi/B_c)^2$ is a minimal resonance width, $\Delta_B = \delta/k_{0F}$, and $B_c \sim D$, where $D \sim (m^* a^2)^{-1}$ is the bandwidth. Thus, B_c corresponds to the field strength that is necessary to reach full spin polarization of the conduction channel.

Varying the temperature, gate voltage, amplitude, and direction of the magnetic field one can achieve four different regimes of thermoelectric transport (Fig. 3, right panel):

(A) $(\Gamma_A,\Gamma_B) \ll T$, fully perturbative NFL regime. While Γ_B is gapped and the gap is $\Gamma_B^{\min} \sim B^2$, Γ_A could be gapless

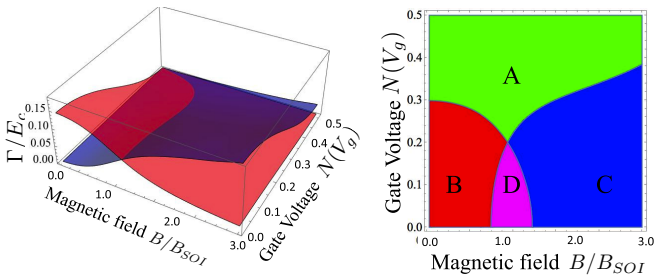

FIG. 3. (Color online) (Left panel) Gate voltage and magnetic field dependence of Γ_α/E_c: red, Γ_A; blue, Γ_B. (Right panel) A "phase diagram" as follows: Four main regimes of the thermoelectric transport are inside the green, red, blue, and magenta domains; A, perturbative NFL, B, weak partial NFL, C, strong partial NFL, D, nonperturbative FL (see details in Sec. VII). Domain boundaries are defined by the crossover condition $\Gamma_A(B,N) = T$ and $\Gamma_B(B,N) = T$. For all plots $\alpha_R = 0.15 v_F$, $\varphi = \pi/4$, $r_0^2 = 0.1$, $k_{0F} L_{\rm QPC} = 3.6$, $T = 0.05 E_c$.

if the gate voltage is fine-tuned to the positions of CB peaks $N \to 1/2$ and $\varphi \to 0$. The TP (34)–(36) demonstrates fingerprints of *weak* NFL logarithmic behavior:

$$S \propto r_0^2 \ln\left(\frac{E_c}{T}\right) \sin(2\pi N). \tag{41}$$

(B) $\Gamma_B \ll T \ll \Gamma_A$, perturbative in Γ_B/T and nonperturbative in Γ_A/T [see (34)–(36)]. This regime can be reached either by fine-tuning the gate voltage away from the CB peaks or by tuning the direction of the Zeeman field to be parallel to SOI in order to suppress the intraband scattering:

$$S \propto \left[|r_+ r_-| \ln\left(\frac{E_c}{T}\right) + |r_\pm r_\mp| \frac{T}{\Gamma_A} \ln\left(\frac{E_c}{\Gamma_A}\right)\right] \sin(2\pi N). \tag{42}$$

The *weak* NFL effects are manifested in the TP log behavior originated from the intraband scattering. The interband processes result in appreciable FL corrections to the TP (34)–(36). The NFL effects are *weak* since the amplitude of intraband scattering is small at $B < B_{\rm SOI}$.

(C) $\Gamma_A \ll T \ll \Gamma_B$, perturbative in Γ_A/T and nonperturbative in Γ_B/T [see (34)–(36)]. This regime is achieved in the vicinity of CB peaks and characterized by *strong NFL* effects due to a weak magnetic field dependence of $|r_\pm|$ and $|r_\mp|$ protected by SOI. Thus, by fine-tuning the orientation of magnetic field perpendicular to SOI $\varphi = 0$ one can controllably protect the NFL behavior of TP in the regime $B < B_{\rm SOI}$. The magnetic field controlled gap associated with the intraband scattering weakly depends on the gate voltage and results in small FL corrections to TP (compared to NFL effects):

$$S \propto \left[|r_+ r_-| \frac{T}{\Gamma_B} \ln\left(\frac{E_c}{\Gamma_B}\right) + |r_\pm r_\mp| \ln\left(\frac{E_c}{T}\right)\right] \sin(2\pi N). \tag{43}$$

(D) $T \ll (\Gamma_A, \Gamma_B)$, FL nonperturbative regime. The NFL logs associated with the intra- and interband scattering processes are cut by the corresponding resonance widths (34)–(36):

$$S \propto T\left[\frac{|r_+ r_-|}{\Gamma_B} \ln\left(\frac{E_C}{\Gamma_B}\right) + \frac{|r_\pm r_\mp|}{\Gamma_A} \ln\left(\frac{E_C}{\Gamma_A}\right)\right] \sin(2\pi N). \tag{44}$$

The TP is a linear function of the temperature. However, the coefficient in front of T strongly depends on both gate voltage and magnetic field.

B. Possible experimental realization and "smoking gun" predictions

Choice of a material. We suggest using narrow-gap semiconductors, e.g., InSb or InAs for the observation of the NFL fingerprints in the quantum transport. Both materials are characterized by large bulk g factors, e.g., $|g| \sim 10$ in InAs (see Ref. [34]) and $|g| \sim 50$ in InSb (see Ref. [35]). The domain of parameters favorable for the observation of the NFL regime is defined as $\delta_0 < T < \gamma B_{\rm SOI} < E_c < \epsilon_F$, where $\delta_0 \sim 1/(\nu_0 V_{\rm QD})$ is a single-particle mean-level spacing in the QD of the size $L_{\rm QD}$ and "volume" $V_{\rm QD}$: $\delta_0^{2D} \sim \hbar^2/(m^* L_{\rm QD}^2)$ and $\delta_0^{3D} \sim (k_F L_{\rm QD})^{-1} \hbar^2/(m^* L_{\rm QD}^2)$, m^* is an effective mass of the carrier in a semiconductor, and other parameters are defined in the previous sections. The condition $L_{\rm QD} < l_{\rm SOI}$ allows one to disregard the effects of the SOI in the QD (Ref. [29]), while the condition $L_{\rm QPC} < l_{mfp}$ defines a ballistic regime of quantum transport through the QPC (here l_{mfp} is an elastic mean-free path).

According to Ref. [35], the parameters for InSb QD-QPC are as follows: $\hbar\alpha_R \sim 0.1$ eV Å $\div$ 0.2 eV Å, $l_{\rm SOI} = \hbar/(m^*\alpha_R) \sim 200$ nm $\div$ 400 nm, $|m^*| \sim 0.015 m_e$ (m_e is electron's mass), $E_{\rm SOI} = m^*\alpha_R^2/2 \sim 50\mu$ eV, the typical charging energy $E_c \sim 1$ meV, and typical Fermi velocities are $\hbar v_F \sim 0.5$ eV Å $\div$ 1 eV Å, while the mean level spacing $\delta_0 < 10\mu$ eV for $L_{\rm QD} \sim l_{\rm SOI}$. The mean-free path of the QPC of a width $d_{\rm QPC} \sim 10$ nm is $l_{mfp} \sim 300$ nm $\div$ 1 μm. Typical parameters for the InAs QD-QPC are not much different [34]: $|m^*| \sim 0.03 m_e$, $\hbar\alpha_R \sim 0.05$ eV Å $\div$ 0.3 eV Å, $l_{\rm SOI} \sim 200$ nm $\div$ 1 μm, and $l_{mfp} \sim 300$ nm $\div$ 1 μm. Therefore, if we assume that $L_{\rm QD} \approx L_{\rm QPC} \sim 300$ nm $\div$ 500 nm, our predictions could be verified at magnetic fields $B < 500$ mT and temperatures $T \sim 100$ mK $\div$ 300 mK for typical densities of 2DEG $n_{\rm 2DEG} \sim 10^{11}$ cm^{-2} $\div$ 10^{12} cm^{-2}. This estimation for parameters is taken from available literature (to our best knowledge), but may vary due to anisotropic character of the g factor which in turn depends on external magnetic field [34] and may also be strongly reduced in confined geometries of the nano-structures.

Testing a Mott-Cutler law. The first important test of the interplay between effects of the SOI and Zeeman field is to verify the Mott-Cutler (MC) law [33] at external in-plane magnetic field. The MC law is a standard benchmark for the FL properties [16]. The MC law says that the TP is proportional to a log derivative of the electric conductance with respect to a position of the chemical potential (gate voltage V_g):

$$S \propto \frac{T}{E_c} \frac{\partial \ln G}{\partial N(V_g)}. \tag{45}$$

In the limit $T \ll (\Gamma_A, \Gamma_B) \ll E_c$ corresponding to the FL regime we get

$$\frac{\partial \ln G}{\partial N(V_g)} \propto E_c\left[\frac{|r_+ r_-|}{\Gamma_B} + \frac{|r_\pm r_\mp|}{\Gamma_A}\right] \sin(2\pi N), \tag{46}$$

while the TP is given by (44). Thus, a strong deviation from the MC law in the FL regime at finite in-plane magnetic fields is a pre-cursor for the NFL behavior discussed in the paper. Notice that break down of the MC law indicates that there exists no equivalent classic electric circuit consisting of the resistances connected in parallel or in series and therefore the effects of both intra- and interband scattering play an important role in the quantum transport. The violation of MC law in the thermoelectric transport through a single-electron transistor have been reported in Ref. [19]. We are not aware of existence of theoretical explanation of this effect in the framework of the FL theory.

Thermopower in the presence of the external B field. The next step is to measure the thermopower of a prototype nanodevice (Fig. 1). The magnitude and orientation of the in-plane magnetic field can be controlled in a standard way by four magnetic coils (not shown in the picture). The TP maximum $eS_{\rm max}(B)$ demonstrates a nonmonotonic magnetic field dependence (strong NFL) which is most pronounced

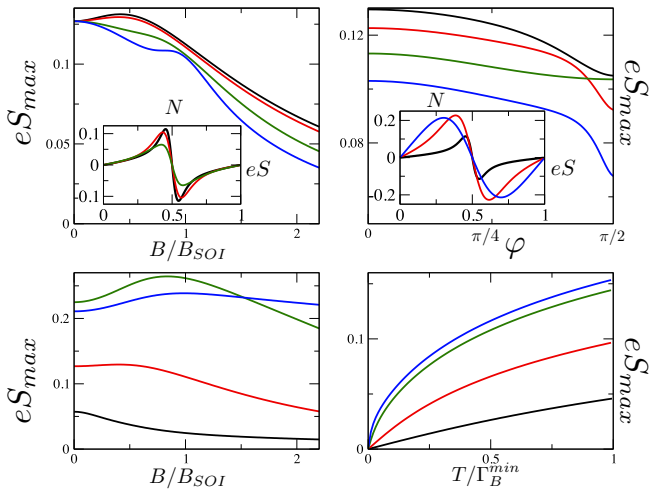

FIG. 4. (Color online) (Top left) $eS_{\max}$ as a function of $B/B_{\rm SOI}$ for different angles φ at $T = 0.001E_c$ and $\alpha_R = 0.15v_F$, from top to bottom $\varphi = \pi/12$, $\pi/6$, $\pi/3$, $5\pi/12$. (Insert) $eS(N)$ for $\varphi = 5\pi/12$ for $B = 0.5B_{\rm SOI}$ (black), $B = B_{\rm SOI}$ (red), $B = 1.5B_{\rm SOI}$ (green). (Top right) $eS_{\max}$ as a function of the angle φ for different amplitudes of $B/B_{\rm SOI}$ at $\alpha_R = 0.15v_F$ and $T = 0.001E_c$ from top to bottom: $B/B_{\rm SOI} = 0.6$, 0.8, 1.0, 1.2. (Insert) $eS(N)$ for $\varphi = 5\pi/12$, $B = 0.5B_{\rm SOI}$, $T = 0.001$ (black), 0.01 (red), 0.1 (blue). (Bottom left) $eS_{\max}$ as a function of $B/B_{\rm SOI}$ for different T/E_c at $\alpha_R = 0.15v_F$ and $\varphi = \pi/6$; $T/E_c = 10^{-1}$, blue (regime A); 10^{-2}, green (crossover $A \to C$); 10^{-3}, red ($B \to D \to C$); 10^{-4}, black ($B \to D$). (Bottom right) $eS_{\max}$ as a function of $T/\Gamma_B^{\min}$ [$\Gamma_B^{\min} = \Gamma_B(1/2)$] with $\alpha_R = 0.15v_F$, $B = 0.5B_{\rm SOI}$, for $\varphi = 5\pi/12$ (black), $\varphi = \pi/3$ (red), $\varphi = \pi/6$ (green), $\varphi = \pi/12$ (blue), ($r_0^2 = 0.1$ and $k_{0F}L_{\rm QPC} = 3.6$).

when $\vec{B}$ is orthogonal to $\vec{B}_{\rm SOI}$ (black curve on Fig. 4, top left and right panels.) This has to be contrasted to almost monotonic TP maximum behavior (blue curves) characteristic for weak NFL-FL regimes. The nonmonotonic behavior of TP maximum as a function of magnetic field is a central prediction of our paper. The nonmonotonicity indicates that the NFL regime of TP is protected by SOI contrast to FL-like behavior demonstrating rapid decrease of TP when magnetic field increases [17]. Another indication of the NFL behavior is attributed to the gate voltage dependence (Fig. 4 inserts). According to [16,17] it is characterized by strongly nonsinusoidal form (Fig. 4 inserts). The TP maximum at zero field, NFL regime, scales according to [16] as $eS_{\max} \sim r_0\sqrt{T/E_c}\ln(E_c/T)$. The TP maximum in the FL regime scales as $eS \sim T/T_{\rm eff}$ with $T_{\rm eff}/E_c = B/B_c \ln^{-1}(B_c/(B|r_0|))$ (Ref. [17]). The B-field dependence of the TP maximum measured at different temperatures (Fig. 4, left bottom panel) allows one to distinguish between four main regimes A–D discussed in the previous subsection. This measurement can be used for identification of crossovers between different domains. The TP maximum depends linearly on T in the FL regime for $T < \Gamma_B^{\min} = \Gamma_B(N = 1/2)$ (Ref. [17]). This regime holds for $\varphi \to \pi/2$. In contrast to the FL regime, the temperature dependence of the TP maximum pronouncedly departs from the linear behavior (see Fig. 4, right bottom panel) when φ is detuned from $\pi/2$. We suggest testing experimentally this effect as a benchmark for the NFL physics.

VIII. SUMMARY AND CONCLUSIONS

We have demonstrated that the theory describing scattering of electrons characterized by two orbital degrees of freedom on a spin $s = 1/2$ quantum impurity (two channel Kondo model) is strongly modified in the presence of both appreciable spin-orbit interaction and Zeeman splitting. It is shown that, on the one hand, the lack of spin conservation due to SOI leads to the appearance of new (extra) scattering channels which potentially enhance the thermoelectric transport. On the other hand, the Zeeman splitting produces nonzero resonance width of Majorana modes describing the quantum impurity and thus suppresses the NFL effects. The interplay between these two tendencies can be controlled by fine-tuning the angle between Zeeman and SOI fields. Our calculations predict a strong dependence of the thermoelectric power on the angle between $\vec{B}$ and $\vec{B}_{\rm SOI}$ and thus open the possibility of controling the scattering mechanism by changing between four, three or two independent scattering processes. While the cases of four and two weak back-scattering do favor the FL behavior, the additional degeneracy in scattering amplitudes appearing for three scattering models due to SOI effects protects the NFL behavior for the range of magnetic fields $B < B_{\rm SOI}$. We conclude therefore, that SOI can indeed protect the NFL against the destructive effects associated with breaking of channel symmetry.

ACKNOWLEDGMENTS

We are grateful to J. C. Egues, V. Fal'ko, L. Glazman, K. Kikoin, A. Komnik, S. Ludwig, C. Marcus, K. Matveev, L. W. Molenkamp, and O. Starykh for illuminating discussions. T.K.T.N. acknowledges support through the short-term visiting program of ICTP. This research in Hanoi is funded by Vietnam National Foundation for Science and Technology Development (NAFOSTED) under the Grant No. 103.01-2014.24.

APPENDIX: EFFECTIVE HAMILTONIAN

1. Backscattering: from fermions to bosons

The backscattering Hamiltonian mixes the left- and right-moving fermions:

$$H_{\rm BS} = v_F \sum_{\lambda\mu\nu} |r_{\mu\nu}|[\Psi^\dagger_{\lambda,\mu}(0)\Psi_{\tilde{\lambda},\nu}(0) + \text{H.c.}]. \qquad \text{(A1)}$$

The Hamiltonians Eqs. (3) and (4) of the main text and the Hamiltonian (A1) can be bosonized [31,32] in terms of dual fields $\phi_\nu(y)$ and $\theta_\nu(y)$ satisfying commutation relations $[\phi_\nu(y),\theta_\mu(y')] = -i\pi\delta_{\nu\mu}\text{sgn}(y - y')/2$ (Refs. [31,32]):

$$\Psi_{\lambda,\nu}(y) = \frac{u_{\lambda,\nu}}{\sqrt{2\pi a}} e^{i\lambda k_F^\nu y} \exp\{i[-\lambda\phi_\nu(y) + \theta_\nu(y)]\}, \qquad \text{(A2)}$$

where $u_{\lambda,\nu}$ are Klein factors [31,32] introduced to ensure proper anticommutation relations between the right- and left-moving fermions.

Using a standard procedure [31,32] we introduce the symmetric (charge) and antisymmetric ("spin") dual variables $\phi_{c,s}(y) = [\phi_+(y) \pm \phi_-(y)]/\sqrt{2}$ and $\theta_{c,s}(y) = [\theta_+(y) \pm \theta_-(y)]/\sqrt{2}$ satisfying the commutation relations

$[\phi_{c/s}(y),\theta_{c/s}(y')] = -i\pi\,\mathrm{sgn}(y-y')/2$ (notice that we still refer to the antisymmetric in the band index bosonic field as "spin"). We rewrite the backscattering Hamiltonian (A1) in terms of the charge and spin bosonic fields as follows:

$$\begin{aligned} H_{\rm BS} = -\frac{2D}{\pi}(&r_s\cos[\sqrt{2}\phi_c(0)]\cos[\sqrt{2}\phi_s(0)] \\ &+ r_a\sin[\sqrt{2}\phi_c(0)]\sin[\sqrt{2}\phi_s(0)] \\ &+ r_{ms}\cos[\sqrt{2}\phi_c(0)]\cos[\sqrt{2}\theta_s(0)] \\ &+ r_{ma}\sin[\sqrt{2}\phi_c(0)]\sin[\sqrt{2}\theta_s(0)]), \end{aligned} \tag{A3}$$

where $r_s = ||r_+| + |r_-||/2$, $r_a = ||r_+| - |r_-||/2$, $r_{ms} = ||r_\pm| + |r_\mp||/2$, $r_{ma} = ||r_\pm| - |r_\mp||/2$.

2. Backscattering: Majorana fermions

As a first step we replace the charge mode by its mean value averaged over fast charge degrees of freedom using the functional integral technique developed in Ref. [16] and obtain the Hamiltonian:

$$\begin{aligned} H_\tau(t) = &\frac{v_F}{2\pi}\int_{-\infty}^{\infty}\{[\partial_y\theta_s(y)]^2 + [\partial_y\phi_s(y)]^2\}dy \\ &-\sqrt{\frac{4D}{v_F}}(\omega_{s\tau}(t)\cos[\sqrt{2}\phi_s(0)] + \omega_{a\tau}(t)\sin[\sqrt{2}\phi_s(0)] \\ &+\omega_{ms\tau}(t)\cos[\sqrt{2}\theta_s(0)] + \omega_{ma\tau}(t)\sin[\sqrt{2}\theta_s(0)]), \end{aligned} \tag{A4}$$

where we use the notations (20) and (21) of the Sec. V.

As a next step we introduce the even and odd combinations of the "spin" (aka sub-band) bosonic fields $\phi_{e/o}(y) = [\phi_s(y) \pm \phi_s(-y)]/\sqrt{2}$, $\theta_{e/o}(y) = [\theta_s(y) \pm \theta_s(-y)]/\sqrt{2}$. As a result, we obtain new chiral fields $\Phi_{1/2}(y) = \theta_{o/e}(y) - \phi_{e/o}(y)$ satisfying the commutation relations: $[\Phi_\alpha(y),\Phi_{\alpha'}(y')] = i\pi\delta_{\alpha\alpha'}\mathrm{sgn}(y-y')$ where $\alpha,\alpha' = 1,2$. We define new fermionic fields $\Psi_\alpha(y) = (\eta_\alpha/\sqrt{2\pi a})\exp(-i\Phi_\alpha(y)$ with a help of two local Majorana fermions $\eta_1 = (d + d^\dagger)/\sqrt{2}$ and $\eta_2 = (d - d^\dagger)/(i\sqrt{2})$ representing the quantum impurity [16].

Finally, we integrate out the fluctuations of the spin degree of freedom with the frequencies exceeding E_c (Ref. [16]). This procedure is equivalent to the poor man's scaling approach originally used for the Kondo problem [36] and leads to replacement of the bandwidth D by the new bandwidth $T_K \sim E_c$. As a result, we derive the effective Anderson model which describes a hybridization of two local Majorana fermions η_1 and η_2 with two species of conduction electrons. The effective Hamiltonian (19) has a structure of two copies of the two-channel Kondo model where coupling constants $\omega_{i\tau}$ depend on both Zeeman and SOI fields:

$$\begin{aligned} H_\tau(t) = \int_{-\infty}^{\infty}dk\Big[&\sum_{\alpha=1,2}(kv_F)c^\dagger_{\alpha,k}c_{\alpha,k} \\ &-\sqrt{2}(\omega_{s\tau}(t)\eta_1(c_{1,k} - c^\dagger_{1,k}) - i\omega_{a\tau}(t)\eta_1(c_{1,k} + c^\dagger_{1,k}) \\ &+\omega_{ms\tau}(t)\eta_2(c_{2,k} - c^\dagger_{2,k}) - i\omega_{ma\tau}(t)\eta_2(c_{2,k} + c^\dagger_{2,k}))\Big]. \end{aligned} \tag{A5}$$

[1] L. D. Landau, Sov. Phys. JETP **3**, 920 (1957); **5**, 101 (1957).
[2] P. W. Anderson, *The Theory of Superconductivity in the High-Tc Cuprate Superconductors* (Princeton University Press, Princeton, 1997).
[3] G. R. Stewart, Rev. Mod. Phys. **73**, 797 (2001).
[4] D. C. Ralph and R. A. Buhrman, Phys. Rev. Lett. **69**, 2118 (1992); D. C. Ralph, A. W. W. Ludwig, J. von Delft, and R. A. Buhrman, *ibid.* **72**, 1064 (1994).
[5] R. M. Potok, I. G. Rau, H. Shtrikman, Y. Oreg, and D. Goldhaber-Gordon, Nature (London) **446**, 167 (2007).
[6] P. Nozieres and A. Blandin, J. Phys. (Paris) **41**, 193 (1980).
[7] A. Zawadowski, Phys. Rev. Lett. **45**, 211 (1980).
[8] A. W. W. Ludwig and I. Affleck, Phys. Rev. Lett. **67**, 3160 (1991).
[9] D. Boese and R. Fazio, Europhys. Lett. **56**, 576 (2001).
[10] T. A. Costi and V. Zlatic, Phys. Rev. B **81**, 235127 (2010).
[11] R. Zitko, J. Mravlje, A. Ramsak, and T. Rejec, New J. Phys. **15**, 105023 (2013).
[12] K. A. Matveev, Phys. Rev. B **51**, 1743 (1995).
[13] K. Flensberg, Phys. Rev. B **48**, 11156 (1993).
[14] A. Furusaki and K. A. Matveev, Phys. Rev. Lett. **75**, 709 (1995); Phys. Rev. B **52**, 16676 (1995).
[15] K. Le Hur, Phys. Rev. B **64**, 161302(R) (2001); K. Le Hur and G. Seelig, *ibid.* **65**, 165338 (2002).
[16] A. V. Andreev and K. A. Matveev, Phys. Rev. Lett. **86**, 280 (2001); K. A. Matveev and A. V. Andreev, Phys. Rev. B **66**, 045301 (2002).
[17] T. K. T. Nguyen, M. N. Kiselev, and V. E. Kravtsov, Phys. Rev. B **82**, 113306 (2010).
[18] S. Amasha, I. G. Rau, M. Grobis, R. M. Potok, H. Shtrikman, and D. Goldhaber-Gordon, Phys. Rev. Lett. **107**, 216804 (2011).
[19] R. Scheibner, H. Buhmann, D. Reuter, M. N. Kiselev, and L. W. Molenkamp, Phys. Rev. Lett. **95**, 176602 (2005).
[20] R. Scheibner, E. G. Novik, T. Borzenko, M. Konig, D. Reuter, A. D. Wieck, H. Buhmann, and L. W. Molenkamp, Phys. Rev. B **75**, 041301 (2007).
[21] R. Winkler, *Spin-Orbit Coupling Effects in Two-Dimensional Electron and Hole Systems* (Springer, Berlin, 2003).
[22] I. Zituc, J. Fabian, and S. Das Sarma, Rev. Mod. Phys. **76**, 323 (2004).
[23] V. Gritsev, G. I. Japaridze, M. Pletyukhov, and D. Baeriswyl, Phys. Rev. Lett. **94**, 137207 (2005).
[24] J. Sun, S. Gangadharaiah, and O. A. Starykh, Phys. Rev. Lett. **98**, 126408 (2007); S. Gangadharaiah, J. Sun, and O. A. Starykh, Phys. Rev. B **78**, 054436 (2008).
[25] R. G. Pereira and E. Miranda, Phys. Rev. B **71**, 085318 (2005).
[26] F. Cheng, K. S. Chan, and K. Chang, New J. Phys. **14**, 013016 (2012).

[27] I. L. Aleiner and L. I. Glazman, Phys. Rev. B **57**, 9608 (1998).
[28] K. Kikoin and Y. Avishai, Phys. Rev. B **86**, 155129 (2012).
[29] I. L. Aleiner and V. I. Fal'ko, Phys. Rev. Lett. **87**, 256801 (2001).
[30] We quantize the conduction electrons in the source using the SOI basis. The FL and tunneling Hamiltonians H_s and $H_{\rm tun}$ preserve the form under a replacement $\sigma \to \nu$.
[31] T. Giamarchi, *Quantum Physics in One Dimension* (Oxford University Press, Oxford, 2004).
[32] A. O. Gogolin, A. A. Nersesyan, and A. M. Tsvelik, *Bosonization and Strongly Correlated Systems* (Cambridge University Press, Cambridge, 2004).
[33] M. Cutler and N. F. Mott, Phys. Rev. **181**, 1336 (1969).
[34] M. D. Schroer, K. D. Petersson, M. Jung, and J. R. Petta, Phys. Rev. Lett. **107**, 176811 (2011).
[35] V. Mourik, K. Zuo, S. M. Frolov, S. R. Plissard, E. P. A. M. Bakkers, and L. P. Kouwenhoven, Science **336**, 1003 (2012).
[36] A. C. Hewson, *The Kondo Problem to Heavy Fermions* (Cambridge University Press, Cambridge, 1993).